



Some Isomers of Nevirapine - A DFT Study

Lemi Türker

Department of Chemistry, Middle East Technical University, Üniversiteler, Eskişehir Yolu No: 1, 06800 Çankaya/Ankara, Turkey; e-mail: lturker@gmail.com; lturker@metu.edu.tr

Abstract

Nevirapine is a dipyridodiazepinone and representative of a new class of anti-HIV agents, the non-nucleoside reverse transcriptase inhibitors. The effect of some centric perturbations on some properties of nevirapine have been investigated within the limitations of density at the level of B3LYP/6-31++G(d,p). The calculations have revealed that the isomers constructed are all thermally favorable and electronically stable. Various calculated properties of the isomers including geometrical, electronic, thermo chemical, quantum chemical and some spectral properties have been harvested and discussed. Additionally, nucleus-independent chemical shift, NICS(0), calculations have been performed and the effect of perturbations on the local aromaticity of six-membered rings have been investigated. The effect of monocentric carbon to nitrogen perturbations on the chemical function descriptors have been determined. Also, the variation of polar surface areas (PSA) of the isomers have been considered in relation to their ability to penetrate the blood-brain barrier.

1. Introduction

Nevirapine (NVP), sold under the brand name Viramune (Figure 1), a dipyridodiazepinone, is a representative of a new class of anti-HIV agents, the non-nucleoside reverse transcriptase (RT) inhibitors [1]. Nevirapine is a potent noncompetitive inhibitor of the retroviral enzyme reverse transcriptase, which is necessary for HIV replication. The agent selectively inhibits HIV-1 but not HIV-2, and it is >8000-fold more selective for infected than uninfected cells [2,3]. Nevirapine inhibits RT by slowing the rate of a magnesium ion-dependent chemical reaction catalyzed by the enzyme [4].

Received: March 19, 2023; Accepted: April 13, 2023; Published: April 18, 2023

Keywords and phrases: nevirapine; Viramune; NVP; anti-HIV agent; density functional.

Copyright © 2023 Lemi Türker. This is an open access article distributed under the Creative Commons Attribution License (<http://creativecommons.org/licenses/by/4.0/>), which permits unrestricted use, distribution, and reproduction in any medium, provided the original work is properly cited.

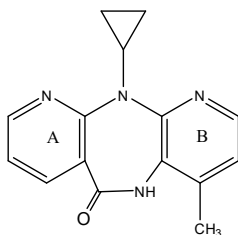


Figure 1. 2D-Structure of nevirapine.

Specifically, nevirapine binding is thought to alter the position of aspartate carboxyl ligands, which results in the slowing of the catalytic reaction rate, but it has no effect on non-nucleoside RT inhibitors. Nevirapine produces a direct stimulatory effect on HIV-I RT ribonuclease (RNase) H activity and alters the cleavage specificity of RNase H [5]. Nevirapine inhibits HIV-I RT RNA- and DNA-dependent DNA polymerase activities in a template-dependent manner. In combination with other antiretroviral agents, nevirapine affords rapid and sustained immunological and virological responses. Triple therapy with zidovudine, didanosine and nevirapine appears to suppress viral replication sufficiently to either prevent or delay the emergence of resistant virus in treatment-naive patients [4]. Palaniappan et al., reported that Nevirapine alters the cleavage specificity of ribonuclease H of human immunodeficiency virus I reverse transcriptase [5]. Although innumerable articles exist in the literature about the medical aspects of Nevirapine, relatively few have appeared on the chemistry, structure, synthesis and other uses of it [6-21].

In the present article, the effect of some centric perturbations on some properties of Nevirapine have been investigated within the limitations of density functional theory and the basis set employed.

2. Method of Calculations

In the present study, all the initial geometry optimizations of the structures leading to energy minima have been achieved by using MM2 method then followed by semi empirical PM3 self-consistent fields molecular orbital (SCF MO) method [22,23] at the restricted level [24]. Afterwards, the structure optimizations have been managed within the framework of Hartree-Fock (HF) and finally by using density functional theory (DFT) at the level of B3LYP/6-31++G(d,p) [25,26]. It is worth mentioning that the exchange term of B3LYP consists of hybrid Hartree-Fock and local spin density (LSD) exchange functions with Becke's gradient correlation to LSD exchange [27]. Also note that the correlation term of B3LYP consists of the Vosko, Wilk, Nusair (VWN3) local correlation

functional [28] and Lee, Yang, Parr (LYP) correlation correction functional [29]. In the present study, the normal mode analysis for each structure yielded no imaginary frequencies for the $3N-6$ vibrational degrees of freedom, where N is the number of atoms in the system. This search has indicated that the structure of each molecule corresponds to at least a local minimum on the potential energy surface. Furthermore, all the bond lengths have been thoroughly searched in order to find out whether any bond cleavage occurred or not during the geometry optimization process. All these computations were performed by using SPARTAN 06 [30]. Whereas the nucleus-independent chemical shift, NICS(0), calculations have been performed by using Gaussian 03 program [31].

3. Results and Discussion

Nevirapine structure was determined by single-crystal X-ray diffraction methods [32]. Nevirapine adopts a “butterfly-like” conformation and is folded such that the angle that subtends the intersecting planes of the pyridine rings is 121° . The cyclopropyl substituent points up and away from the molecular framework of the tricyclic system, with the plane of the cyclopropyl ring being almost perpendicular to the pseudoplane of the boat conformation of the 7-membered ring (diazepinone) [32].

Figure 2 shows the optimized structures (at the level of B3LYP/6-31++G(d,p)) of the presently considered isomers of nevirapine. Direction of the calculated dipole moment

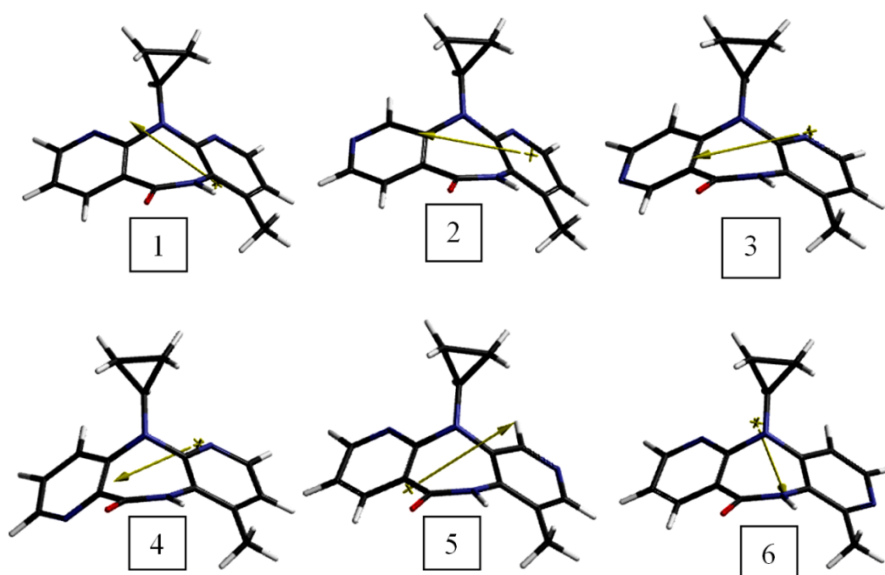


Figure 2. Optimized structures of the isomers considered.

vectors are also shown. Note that the isomers of present concern have been engendered starting from nevirapine, by means of carbon to nitrogen (or vice versa) monocentered perturbations at a time, in ring-A of nevirapine to produce isomeric set of structures 1-4. Then the similar type perturbations are made in ring-B, keeping ring-A of nevirapine as it is to produce isomeric structures-5 and 6 (such that only one nitrogen atom exists either of the six-membered rings). As the perturbations occur, the magnitude (see Table 1) as well as direction of the dipole moment vectors change. Except the cases of isomers-5 and 6, generally the dipole moment originates somewhere nearby the methyl-substituted pyridyl ring.

Table 1 tabulates some calculated properties of the isomers considered. The order of dipole moments is $3 > 4 > 2 > 1 > 6 > 5$. Thus, isomers-3 and 5 possess the largest and the smallest dipole moment values, respectively. Note that the applied perturbations mainly affect the dipole moments and log P values.

Table 1. Some properties of the isomers considered.

Isomer	Dipole moment	Polarizability	Area (Å ²)	Volume (Å ³)	Ovality	Log P
1	2.53	62.17	281.71	269.24	1.40	0.13
2	4.36	62.18	279.89	268.88	1.39	-1.03
3	5.35	62.07	279.33	268.66	1.39	-1.03
4	4.53	62.14	281.28	269.23	1.39	-1.37
5	0.34	62.16	279.45	268.75	1.39	-1.03
6	2.34	62.12	279.82	268.81	1.39	-0.43

Dipole moments in debye units. Polarizabilities in 10^{-30} m³ units.

On the other hand, the polarizability is defined according to the multi variable formula [30].

$$\text{Polarizability} = 0.08 * V - 13.0353 * h + 0.979920 * h^2 + 41.3791$$

where V and h are the Van der Waals volume and hardness, respectively. Hardness is defined as,

$$\text{Hardness} = -(\epsilon_{\text{HOMO}} - \epsilon_{\text{LUMO}})/2$$

where ϵ_{HOMO} and ϵ_{LUMO} are the molecular orbital energies of the highest occupied (HOMO) and the lowest unoccupied (LUMO) molecular orbital energies.

Table 2 shows aqueous and solvation energies of the isomers considered. The algebraic order of calculated aqueous energies is $1 < 6 < 3 < 5 < 2 < 4$. Whereas the solvation energies follow the order of $4 < 3 < 5 < 2 < 1 < 6$. Note that the solvation order arises from the intricate function of various factors listed in Table 1.

Table 2. E_{aq} and E_{sol} energies of the isomers considered.

	1	2	3	4	5	6
E_{aq}	-2295504.91	-2295484.98	-2295496.01	-2295477.45	-2295493.85	-2295498.76
E_{sol}	-36.04	-37.92	-39.48	-41.50	-38.57	-35.94

E_{aq} : Aqueous energy, E_{sol} : Solvation energy. Energies in kJ/mol.

The log P values, except structure-1 (nevirapine) are all negative quantities. The order is $1 > 6 > 2 = 3 = 5 > 4$. Note that and hydrophilic drugs (having low octanol/water partition coefficients) are found primarily in aqueous regions.

In Table 3 some thermo chemical values of the considered isomers are tabulated. As seen in the table, all the structures have exothermic heat of formation and favorable Gibb's free energy of formation values at the standard state. The orders of H° and G° values are the same as $1 < 6 < 3 < 5 < 2 < 4$, so nevirapine is the most exothermic and the most favorable structure among of all.

Table 3. Some thermo chemical values of the isomers considered.

Isomer	H°	S° (J/mol $^\circ$)	G°
1	-2294741.840	479.89	-2294884.921
2	-2294720.048	480.43	-2294863.289
3	-2294728.870	480.28	-2294872.066
4	-2294709.966	480.69	-2294853.286
5	-2294727.179	480.01	-2294870.297
6	-2294735.156	479.48	-2294878.113

Energies in kJ/mol.

The electrostatic potential (ESP) charges on atoms of the tautomers are depicted in Figure 3. Note that the ESP charges are obtained by the program based on a numerical method that generates charges that reproduce the electrostatic potential field from the entire wavefunction [30].

Table 4 shows the ESP charges on N-atoms of rings -A and B of the isomers 1-6. The algebraic orders of the ESP charges on N-atoms of rings -A and B are $5 < 3 < 6 < 2 < 1 < 4$ and $6 < 4 < 2 < 3 < 1 < 5$, respectively.

Figure 4 illustrates the electrostatic potential maps of the isomers considered. The red/orange regions stand for negative whereas the blue regions for positive charge/potential development. In the isomers considered the negative region coincides mainly with the lactam carbonyl moiety whereas the positive region overlaps with the lactam NH moiety. Note that the lone pair of that lactam nitrogen atom is in conjugation with the carbonyl group as well as with the pyridyl ring. In isomer-4 the pyridyl nitrogen is in conjugation with the lactam moiety through the π -skeleton.

Table 5 shows some energies of the isomers considered where E , ZPE and E_C stand for the total electronic energy, zero point vibrational energy and the corrected total electronic energy, respectively. The data reveal that all the structures considered are electronically stable. The stability order is $1 > 6 > 3 > 5 > 2 > 4$ which follows the order of G° values.

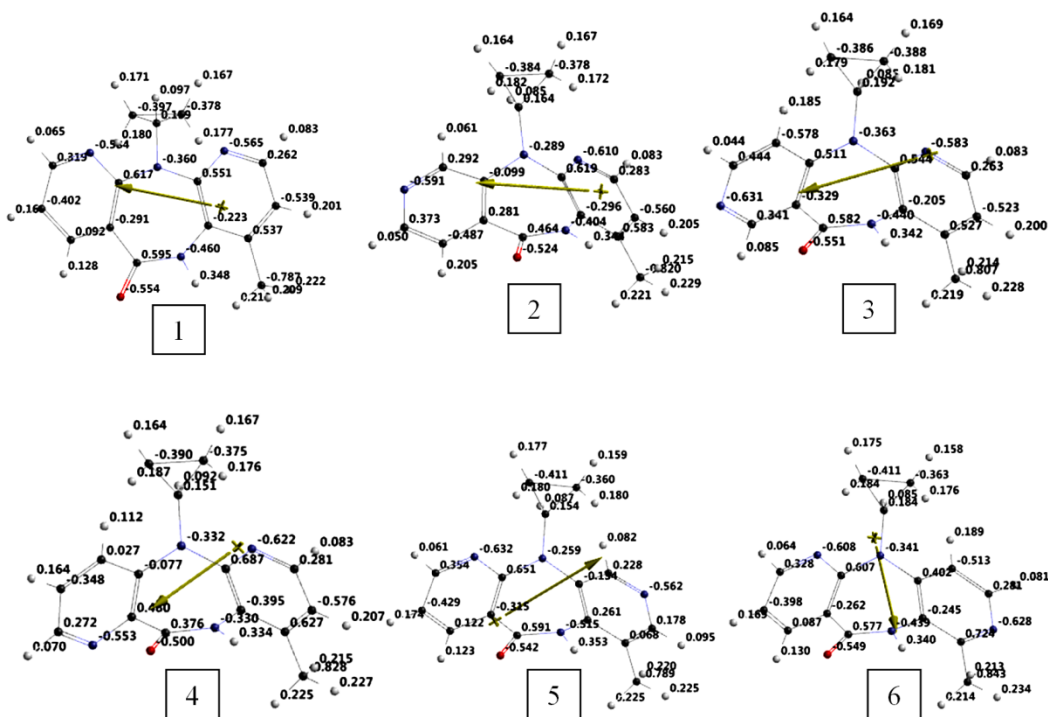
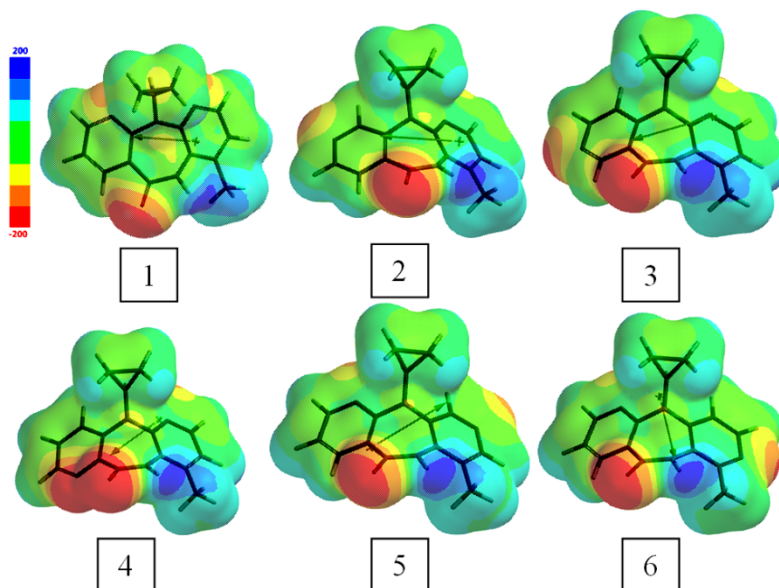


Figure 3. Electrostatic potential charges on atoms of the isomers considered.

Table 4. ESP charges on N-atoms of rings A and B of the isomers 1-6.

1	2	3	4	5	6
-0.584	-0.591	-0.631	-0.553	-0.632	-0.608
-0.565	-0.610	-0.583	-0.622	-0.562	-0.628

In each row the first and second entries stand for ring-A and ring-B of the isomers.

**Figure 4.** Electrostatic potential maps of the isomers considered.**Table 5.** Some energies of the isomers considered.

Isomer	E	ZPE	E _C
1	-2295468.87	709.28	-2294759.59
2	-2295447.06	709.20	-2294737.86
3	-2295456.53	709.87	-2294746.66
4	-2295435.95	708.07	-2294727.88
5	-2295455.28	710.36	-2294744.92
6	-2295462.82	709.97	-2294752.85

Energies in kJ/mol.

The HOMO, LUMO energies and intermolecular orbital energy gap ($\Delta\epsilon$) values of the isomers are shown in Table 6. As seen in the table the HOMO and LUMO orders are 3<6<5<2<4<1 and 5<2<6<1<3<4, respectively. So, all the perturbations lower the HOMO energies at different extents as compared to nevirapine. The effect on the LUMO energies is not so simple that is depending on the position of the perturbation, some lower and some raise the LUMO energy as compared to nevirapine. As the perturbation occurs in ring-A, the HOMO order variation is 3<2<4<1 whereas in ring-B it is 6<5<1. As for the LUMO orders, the variations in rings A and B, affect the LUMO energies in the order of 2<1<3<4 and 5<6<1, respectively. So, the most dramatic energy lowering effect of the perturbation on the HOMO energy occurs at position-3. Note that the gross and fine topologies of the structures are controlling factors on lowering and raising of the molecular orbital energies. As for the $\Delta\epsilon$ values, the order is 3>4>6>1>5>2.

Table 6. The HOMO, LUMO energies and $\Delta\epsilon$ values of the isomers considered.

Isomer	HOMO	LUMO	$\Delta\epsilon$
1	-592.03	-166.87	425.16
2	-594.57	-183.35	411.22
3	-608.86	-162.89	445.97
4	-593.74	-153.86	439.88
5	-598.49	-183.58	414.91
6	-609.38	-177.46	431.92

Energies in kJ/mol.

The isomers absorb mainly in the UV region, and the spectra slightly intrude the visible region. Table 7 tabulates the λ_{\max} values and Figure 5 shows some typical UV-VIS spectrums of the isomers.

Table 7. λ_{\max} values of the isomers.

1	2	3	4	5	6
273.61	265.11	252.75	273.66	262.42	273.85
339.60	356.61	-	328.03	350.75	334.07

λ_{\max} values in nm. The first entry in each row stands for the main absorption value.

Figure 6 is the local ionization potential map of nevirapine isomers considered, where conventionally red/reddish regions (if any exists) on the density surface indicate areas from which electron removal is relatively easy, meaning that they are subject to electrophilic attack.

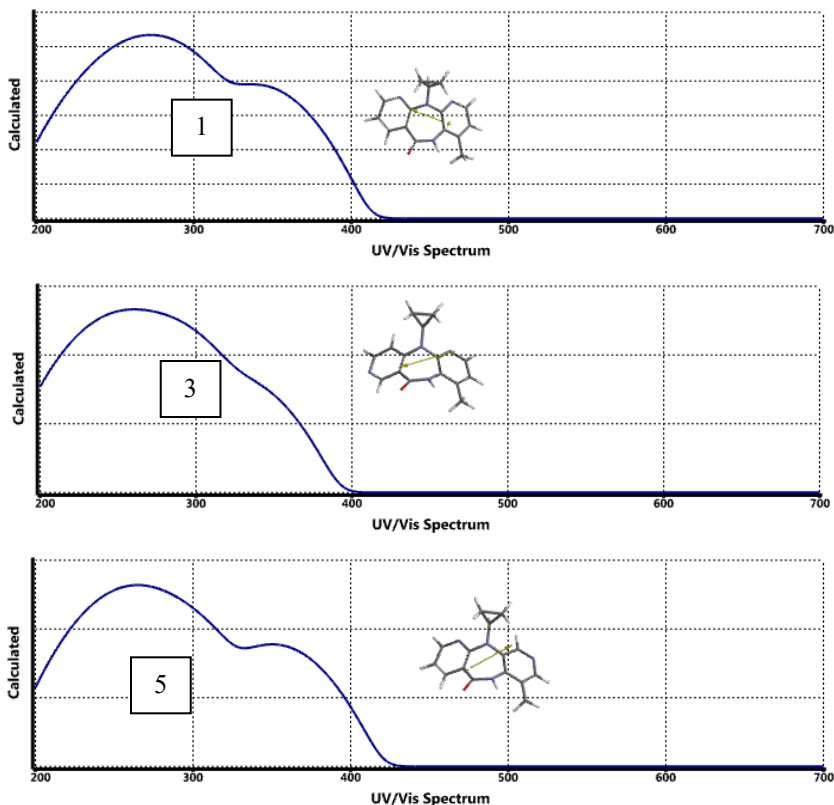
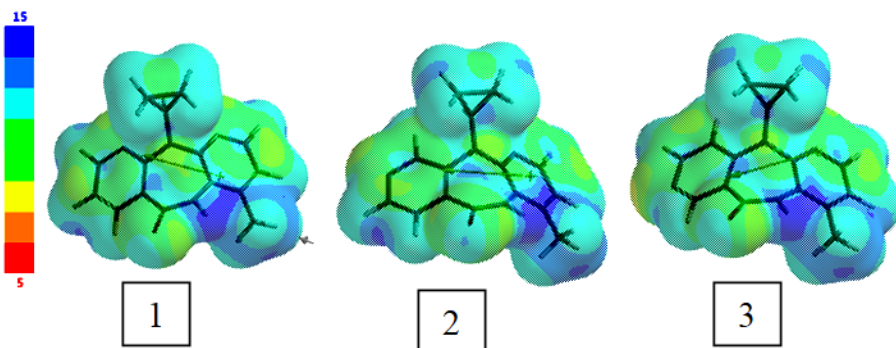


Figure 5. Some of the calculated UV-VIS spectra of the isomers.



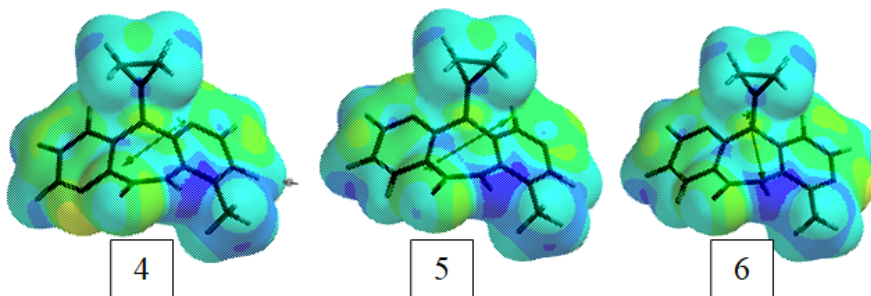


Figure 6. The local ionization potential maps of the isomers considered.

Figure 7 shows the LUMO maps of nevirapine isomers considered. Note that a LUMO map displays the absolute value of the LUMO on the electron density surface. The blue color (if any exists) stands for the maximum value of the LUMO and the red colored region, associates with the minimum value.

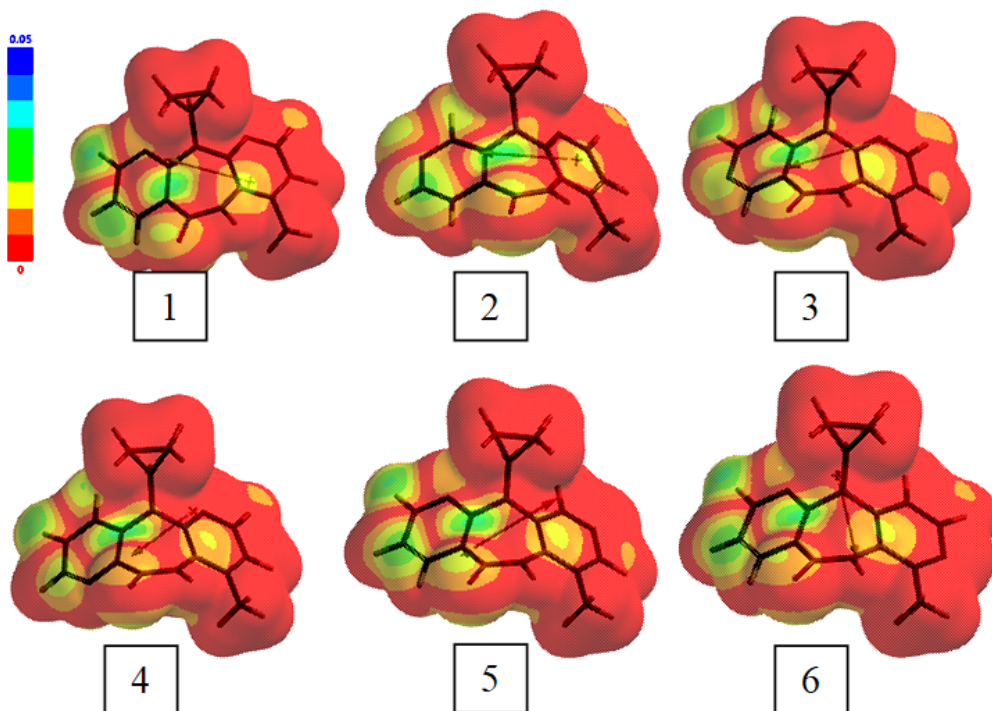


Figure 7. The LUMO maps of the isomers considered.

In Figure 8, structures 1-6 show the effect of monocentric carbon to nitrogen perturbations on the chemical function descriptors (CFD) of the isomers considered. Note that CFDs are attributes given to a molecule in order to characterize or anticipate its chemical behavior. In the figure the blue regions on the molecules stand for hydrophobe, greens for hydrogen bond acceptor, pale purple ones for hydrogen bond donor/acceptor and positive ionizable sites, respectively. In all the cases cyclopropyl ring keeps its hydrophobic character but six-membered rings exhibit different behavior throughout the perturbation process. The lactam moiety keeps its character be the same in all the cases.

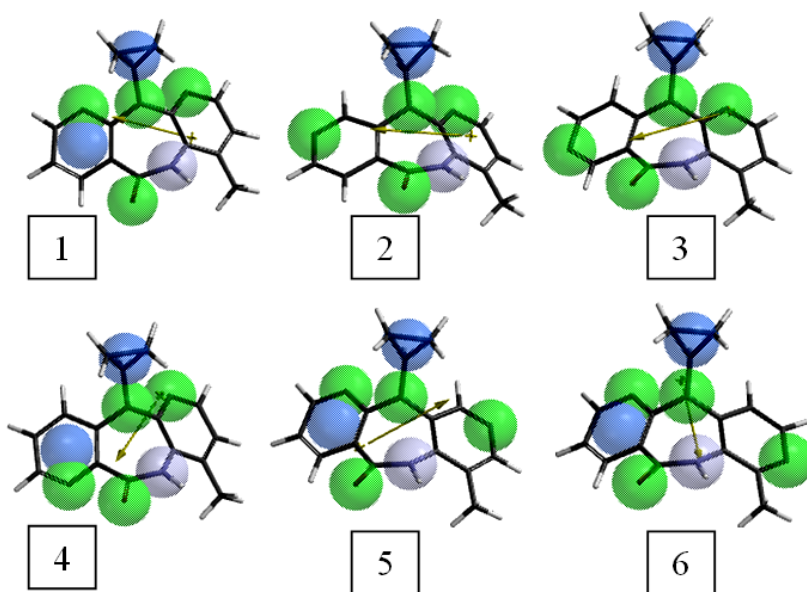


Figure 8. CFDs of the isomers considered.

Note that solvation is dictated by the intricate function of various factors which are particular characteristics of the solute and the solvent, such as the cavity energy, orientation energy, isotropic and anisotropic interaction energies, etc. [33]. Table 8 lists polar surface areas (PSA) of the isomers considered. It is defined as the amount of molecular surface area arising from polar atoms (N,O) together with their attached hydrogen atoms. Molecules with PSA values greater than 140 \AA^2 tend to be poor at permeating cell membranes to penetrate. To penetrate the blood-brain barrier a PSA value of a molecule should be less than 90 \AA^2 [34,35]. As seen in the table, all of the isomers considered possess PSA values comparable to the value of nevirapine. The order is $1 < 6 < 5 < 2 < 3 < 4$.

Table 8. The PSA (\AA^2) values of the isomers considered.

1	2	3	4	5	6
37.136	38.463	38.494	38.768	38.086	38.015

NICS

Nucleus independent chemical shifts (NICS) is the computed value of the negative magnetic shielding at some selected point in space. It gives an idea about the local aromaticity of a ring or cage. Generally it is calculated at center of a ring or cage (NICS(0)). Through the years, numerous articles have appeared in the literature, discussing aromaticity in terms of energetic, structural and magnetic criteria [36-47]. Positive NICS values stand for antiaromaticity (28.8 for cyclobutadiene) while small NICS values are associated with non-aromaticity (-2.1 for cyclohexane, -1.1 for adamantane). On the contrary, negative NICS values denote aromaticity (such as -11.5 for benzene, -11.4 for naphthalene). However, it is to be mentioned that although NICS approach has been proved to be an effective probe for the local aromaticity of individual rings of polycyclic systems, a couple of contradictory results exist [47].

Table 8 shows the NICS(0) values for the presently considered isomers of nevirapine. The order of the NICS values are $6 < 4 < 2 < 5 < 3 < 1$ and $6 < 5 < 4 < 3 < 1 < 2$, respectively for A and B rings. As seen in the table, the perturbations generally yield more aromatic B-ring compared to ring-A. The cause of it probably due to the direct conjugation of the carbonyl group (attracts electrons) with ring-A whereas the methyl group inductively donates some electron pool to ring-B.

Table 8. NICS values of rings A and B of the isomers considered.

Isomer	A	B
1	-6.3998	-7.3137
2	-7.1049	-7.2821
3	-6.5368	-7.3710
4	-7.3825	-7.4020
5	-6.6487	-7.6584
6	-7.6662	-7.6662

See Figure 1 for labeling of the rings.

4. Conclusion

Within the limitations of the theory and basis set used, the present DFT treatment has indicated that in vacuum and aqueous conditions, the isomers considered are electronically stable and have thermo chemically favorable formation values. The type of perturbations considered in the present article are effective at different extents on certain properties of the isomers as compared to nevirapine. Obviously their extents are dictated by the gross and fine topology of the backbone of the structures considered. Since, nevirapine is a potent noncompetitive inhibitor of the retroviral enzyme reverse transcriptase, which is necessary for HIV replication, some of the isomers considered presently might have some medical applicability because they have some properties comparable with those of nevirapine. Thus, they might be some candidates for worth testing further.

References

- [1] Grozinger, K., Proudfoot, J., & Hargrave, K. (2006). Discovery and development of nevirapine. In M.S. Chorghade (Ed.). *Drug discovery and development: Drug discovery* (V. 1, Ch.13, pp. 353-363). NY: Wiley. <https://doi.org/10.1002/0471780103.ch13>
- [2] Patel, S.S., & Benfield, P. (1996). Nevirapine. *Clin. Immunother.*, 6(4), 307-317. <https://doi.org/10.1007/BF03259093>
- [3] Milinkovic, A., & Martinez, E. (2004). Nevirapine in the treatment of AIDS, *Experts. Rev. Anri-infect. Ther.*, 2(3), 367-373. <https://doi.org/10.1586/14787210.2.3.367>
- [4] Spence, R.A., Kati, W.M., Anderson, K.S., & Johnson, K.A. (1995). Mechanism of inhibition of HIV-I reverse transcriptase by nonnucleoside inhibitors. *Science*, 267, 988-93. <https://doi.org/10.1126/science.7532321>
- [5] Palaniappan, C., Fay, P.J., & Bambara, R.A. (1995). Nevirapine alters the cleavage specificity of ribonuclease H of human immunodeficiency virus I reverse transcriptase. *J. Bioi. Chem.*, 270(9), 4861-9. <https://doi.org/10.1074/jbc.270.9.4861>
- [6] Mui, P.W., Jacober, S.P., Hargrave, K.D., & Adams, J. (1992). Crystal structure of nevirapine, a non-nucleoside inhibitor of HIV-1 reverse transcriptase, and computational alignment with a structurally diverse inhibitor. *Journal of Medicinal Chemistry*, 35(1), 201-202. <https://doi.org/10.1021/jm00079a029>
- [7] Caira, M.R., Stieger, N., Liebenberg, W., De Villiers, M.M., & Samsodien, H. (2008). Solvent inclusion by the anti-HIV drug nevirapine: X-ray structures and thermal decomposition of representative solvates. *Crystal Growth & Design*, 8(1), 17-23. <https://doi.org/10.1021/cg070522r>

- [8] Burke, E.W.D., Morris, G.A., Vincent, M.A., Hillier, I.H., & Clayden, J. (2012). Is nevirapine atropisomeric? Experimental and computational evidence for rapid conformational inversion. *Org. Biomol. Chem.*, 10, 716-719. <https://doi.org/10.1039/C1OB06490H>
- [9] Diab, S., McQuade, D.T., Gupton, B.F., & Gerogiorgis, D.I. (2019). Process design and optimization for the continuous manufacturing of nevirapine, an active pharmaceutical ingredient for HIV treatment. *Organic Process Research & Development*, 23(3), 320-333. <https://doi.org/10.1021/acs.oprd.8b00381>
- [10] Sylvain, B., Defoy, D., Dory, Y.L., & Klarskov, K. (2009). Efficient synthesis of nevirapine analogs to study its metabolic profile by click fishing. *Bioorganic & Medicinal Chemistry Letters*, 19(21), 6127-6130. <https://doi.org/10.1016/j.bmcl.2009.09.011>
- [11] Sharma, A.M., Klarskov, K., & Uetrecht, J. (2013). Nevirapine bioactivation and covalent binding in the skin. *Chemical Research in Toxicology*, 26(3), 410-421. <https://doi.org/10.1021/tx3004938>
- [12] Bhat, J.I., & Alva, V.D.P. (2011). Inhibition effect of nevirapine an antiretroviral on the corrosion of mild steel under acidic condition. *Journal of the Korean Chemical Society*, 55(5), 835-841. <https://doi.org/10.5012/JKCS.2011.55.5.835>
- [13] Bhembe, Y.A., Lukhele, L.P., Hlekelele, L., Ray, S.S., Sharma, A., Vo, D-V.N., & Dlamini, L.N. (2020). Photocatalytic degradation of nevirapine with a heterostructure of few-layer black phosphorus coupled with niobium (V) oxide nanoflowers (FL BP@Nb₂O₅). *Chemosphere*, 261, 128159. <https://doi.org/10.1016/j.chemosphere.2020.128159>
- [14] Apath, D., Moyomailto:moyom@staff.msu.ac.zw<https://orcid.org/0000-0003-4845-3028>, M., & Shumba, M. (2020). TiO₂ nanoparticles decorated graphene nanoribbons for voltammetric determination of an anti-HIV drug nevirapine. *Journal of Chemistry*, 2020, Article ID 3932715, 13 pp. <https://doi.org/10.1155/2020/3932715>
- [15] Tateishi, Y., Ohe, T., Yasuda, D., Takahashi, K., Nakamura, S., Kazuki, Y., & Mashino, T. (2020). Synthesis and evaluation of nevirapine analogs to study the metabolic activation of nevirapine. *Drug Metabolism and Pharmacokinetics*, 35(2), 238-243, <https://doi.org/10.1016/j.dmpk.2020.01.006>
- [16] Sathisaran, I., & Dalvi, S.V. (2021). Cocrystallization of an antiretroviral drug nevirapine: an eutectic, a cocrystal solvate, and a cocrystal hydrate. *Crystal Growth & Design*, 21(4), 2076-2092. <https://doi.org/10.1021/acs.cgd.0c01513>

- [17] Ayala, A.P., Siesler, H.W., Wardell, S.M.S.V., Boechat, N., Dabbene, V., & Cuffni, S.L. (2007). Vibrational spectra and quantum mechanical calculations of antiretroviral drugs: Nevirapine. *J. Mol. Struct.*, 828(1-3), 201-210. <https://doi.org/10.1016/j.molstruc.2006.05.055>
- [18] Vailikhit, V., Bunsawansong, P., Techasakul, S., & Hannongbua, S. (2006). Conformational analysis of nevirapine in solutions based on nmr spectroscopy and quantum chemical calculations. *J. Theor. Comput. Chem.*, 5(4), 913-924. <https://doi.org/10.1142/S0219633606002702>
- [19] Parreira, R.L.T., Abrahão-Júnior, O., & Galembeck, S.E. (2001). Conformational preferences of non-nucleoside HIV-1 reverse transcriptase inhibitors. *Tetrahedron*, 57(16), 3243-3253. [https://doi.org/10.1016/S0040-4020\(01\)00193-4](https://doi.org/10.1016/S0040-4020(01)00193-4)
- [20] Abrahão-Júnior, O., Nascimento, P.G.B.D., & Galembeck, S.E. (2001). Conformational analysis of the HIV-1 virus reverse transcriptase nonnucleoside inhibitors: TIBO and nevirapine. *J. Comput. Chem.*, 22(15), 1817-1829. <https://doi.org/10.1002/jcc.1133>
- [21] Hannongbua, S., Prasithichokekul, S., & Pungpo, P.(2001). Conformational analysis of nevirapine, a non-nucleoside HIV-1 reverse transcriptase inhibitor, based on quantum mechanical calculations. *J. Comput. Aided Mol. Des.*, 15, 997-1004. <https://doi.org/10.1023/A:1014881723431>
- [22] Stewart, J.J.P. (1989). Optimization of parameters for semi empirical methods I. *J. Comput. Chem.*, 10, 209-220. <https://doi.org/10.1002/jcc.540100208>
- [23] Stewart, J.J.P. (1989). Optimization of parameters for semi empirical methods II. *J. Comput. Chem.*, 10, 221-264. <https://doi.org/10.1002/jcc.540100209>
- [24] Leach, A.R. (1997). *Molecular modeling*. Essex: Longman.
- [25] Kohn, W., & Sham, L.J. (1965). Self-consistent equations including exchange and correlation effects. *Phys. Rev.*, 140, 1133-1138. <https://doi.org/10.1103/PhysRev.140.A1133>
- [26] Parr, R.G., & Yang, W. (1989). *Density functional theory of atoms and molecules*. London: Oxford University Press.
- [27] Becke, A.D. (1988). Density-functional exchange-energy approximation with correct asymptotic behavior. *Phys. Rev. A*, 38, 3098-3100. <https://doi.org/10.1103/PhysRevA.38.3098>
- [28] Vosko, S.H., Wilk, L., & Nusair, M. (1980). Accurate spin-dependent electron liquid correlation energies for local spin density calculations: a critical analysis. *Can. J. Phys.*, 58, 1200-1211. <https://doi.org/10.1139/p80-159>

- [29] Lee, C., Yang, W., & Parr, R.G. (1988). Development of the Colle-Salvetti correlation energy formula into a functional of the electron density. *Phys. Rev. B*, 37, 785-789. <https://doi.org/10.1103/PhysRevB.37.785>
- [30] SPARTAN 06 (2006). Wavefunction Inc. Irvine CA, USA.
- [31] Gaussian 03, Frisch, M.J., Trucks, G.W., Schlegel, H.B., Scuseria, G.E., Robb, M.A., Cheeseman, J.R., Montgomery, Jr., J.A., Vreven, T., Kudin, K.N., Burant, J.C., Millam, J.M., Iyengar, S.S., Tomasi, J., Barone, V., Mennucci, B., Cossi, M., Scalmani, G., Rega, N., Petersson, G.A., Nakatsuji, H., Hada, M., Ehara, M., Toyota, K., Fukuda, R., Hasegawa, J., Ishida, M., Nakajima, T., Honda, Y., Kitao, O., Nakai, H., Klene, M., Li, X., Knox, J.E., Hratchian, H.P., Cross, J.B., Bakken, V., Adamo, C., Jaramillo, J., Gomperts, R., Stratmann, R.E., Yazyev, O., Austin, A.J., Cammi, R., Pomelli, C., Ochterski, J.W., Ayala, P.Y., Morokuma, K., Voth, G.A., Salvador, P., Dannenberg, J.J., Zakrzewski, V.G., Dapprich, S., Daniels, A.D., Strain, M.C., Farkas, O., Malick, D.K., Rabuck, A.D., Raghavachari, K., Foresman, J.B., Ortiz, J.V., Cui, Q., Baboul, A.G., Clifford, S., Cioslowski, J., Stefanov, B.B., Liu, G., Liashenko, A., Piskorz, P., Komaromi, I., Martin, R.L., Fox, D.J., Keith, T., Al-Laham, M.A., Peng, C.Y., Nanayakkara, A., Challacombe, M., Gill, P.M.W., Johnson, B., Chen, W., Wong, M.W., Gonzalez, C., & Pople, J.A., Gaussian, Inc., Wallingford CT, 2004.
- [32] Mui, P.W., Jacober, S.P., Hargrave, K.D., & Adams, J. (1992). Crystal structure of nevirapine, a non-nucleoside inhibitor of HIV-1 reverse transcriptase, and computational alignment with a structurally diverse inhibitor. *Journal of Medicinal Chemistry*, 35(1), 201-202. <https://doi.org/10.1021/jm00079a029>
- [33] Reichardt, C. (2004). *Solvent effects and solvent effects in organic chemistry*. Weinheim: Wiley-VCH.
- [34] Hitchcock, S.A., & Pennington, L.D. (2006). Structure-brain exposure relationships. *J. Med. Chem.*, 49(26), 7559-7583. <https://doi.org/10.1021/jm060642i>. PMID 17181137.
- [35] Shityakov, S., Neuhaus, W., Dandekar, T., & Förster, C. (2013). Analysing molecular polar surface descriptors to predict blood-brain barrier permeation. *International Journal of Computational Biology and Drug Design*, 6(1-2), 146-56. <https://doi.org/10.1504/IJCBDD.2013.052195>. PMID 23428480.
- [36] Minkin, V.I., Glukhovtsev, M.N., & Simkin, B.Y. (1994). *Aromaticity and antiaromaticity: Electronic and structural aspects*. New York: Wiley.
- [37] Schleyer, P.R., & Jiao, H. (1996). What is aromaticity?. *Pure Appl. Chem.*, 68, 209-218. <https://doi.org/10.1351/pac199668020209>

- [38] Glukhovtsev, M.N. (1997). Aromaticity today: energetic and structural criteria. *J. Chem. Educ.*, *74*, 132-136. <https://doi.org/10.1021/ed074p132>
- [39] Krygowski, T.M., Cyranski, M.K., Czarnocki, Z., Hafelinger, G., & Katritzky, A.R. (2000). Aromaticity: a theoretical concept of immense practical importance. *Tetrahedron*, *56*, 1783-1796. [https://doi.org/10.1016/s0040-4020\(99\)00979-5](https://doi.org/10.1016/s0040-4020(99)00979-5)
- [40] Schleyer, P.R. (2001). Introduction: aromaticity. *Chem. Rev.*, *101*, 1115-1118. <https://doi.org/10.1021/cr0103221>
- [41] Cyranski, M.K., Krygowski, T.M., Katritzky, A.R., & Schleyer, P.R. (2002). To what extent can aromaticity be defined uniquely?. *J. Org. Chem.*, *67*, 1333-1338. <https://doi.org/10.1021/jo016255s>
- [42] Chen, Z., Wannere, C.S., Corminboeuf, C., Puchta, R., & Schleyer, P. von R. (2005). Nucleus independent chemical shifts (NICS) as an aromaticity criterion. *Chem. Rev.*, *105*(10), 3842-3888. <https://doi.org/10.1021/cr030088>
- [43] Gershoni-Poranne, R., & Stanger, A. (2015). Magnetic criteria of aromaticity. *Chem. Soc.Rev.*, *44*(18), 6597-6615. <https://doi.org/10.1039/c5cs00114e>
- [44] Dickens, T.K., & Mallion, R.B. (2016). Topological ring-currents in conjugated systems. *MATCH Commun. Math. Comput. Chem.*, *76*, 297-356.
- [45] Stanger, A. (2010). Obtaining relative induced ring currents quantitatively from NICS. *J. Org. Chem.*, *75*(7), 2281-2288. <https://doi.org/10.1021/jo1000753>
- [46] Monajjemi, M., & Mohammadian, N.T. (2015). S-NICS: An aromaticity criterion for nano molecules. *J. Comput. Theor. Nanosci.*, *12*(11), 4895-4914. <https://doi.org/10.1166/jctn.2015.4458>
- [47] Schleyer, P.R., Maerker, C., Dransfeld, A., Jiao, H., & Hommes, N.J.R.E. (1996). Nucleus independent chemical shifts: a simple and efficient aromaticity probe. *J. Am. Chem. Soc.*, *118*(26), 6317-6318. <https://doi.org/10.1021/ja960582d>. PMID: 28872872.